New Magnet Design for Fast-Field-Cycling Nuclear Magnetic Resonance

Stephan Kruber, Germán D. Farrher and E. Anoardo, *Member,* IEEE

***Abstract*— A new magnet design for fast-field-cycling nuclear magnetic resonance is described. A topic of interest is the compensation of the magnetic field homogeneity during the generation of the pulsed magnetic field. In contrast with previous solutions, the magnet system here discussed can be electronically controlled. In Kelvin-type magnets used today, the homogeneity of the field is set-up through a current density distribution along the air-cored cylinders that compose the magnet coil. A common feature of this type of magnets is that the magnetic field value and its homogeneity are affected by thermo-mechanical stress during the strong current pulses applied to the coil. In the new design here presented, the problem can be circumvented through a multicoil arrangement driven by individual current sources, allowing an automatic correction of the magnetic field drift and the homogeneity.**

***Keywords*— magnet, fast-field-cycling, homogeneity, nuclear magnetic resonance.**

I. Introduction

DURING the last decades the Nuclear Magnetic Resonance (NMR) fast-field-cycling (FFC) technique has developed to an important technique for scientific use [1]-[3]. It has also turned into a new approach in Magnetic Resonance Imaging [4]-[8]. One of the crucial parts of any fast-field-cycling device is the magnet system. It determines the characteristics of the whole apparatus and therewith its application range. The technical demands on the magnetic field generator for a FFC apparatus are strongly correlated among themselves, which makes an optimisation of each, at the same time, almost impractical. One of these demands is to achieve a maximal magnetic flux density from an applied electrical power P. Another is to obtain an adequate homogeneity $\Delta B / B$ over a desired volume, as well as to accomplish fast variation rates of the magnetic flux density (dB / dt). The optimisation problem arises from the fact that high magnetic flux densities together with a good homogeneous spatial distribution require large coil volumes, a high quantity of windings and therefore high inductances. In turn, fast variation rates of the magnetic flux density need low inductances, which are achieved by minimizing the dimensions of the coil as well as the quantity of windings. This is contradictory and can only lead to compromises between these requirements. Due to that, air-core magnets comprised of non- ferromagnetic materials are used in fast-field-cycling devices in order to avoid the low frequency response and the high hysteresis loops of ferromagnetic materials. Moreover other considerations have to be taken into account. The resistance of the magnetic system is of high importance as well. First, low resistances will result in lower power dissipation in the magnetic system, thus making it easier to reduce the temperature fluctuations and thermo-mechanical stress of the magnet. Second, the resistance is also affecting the variation rates of the magnetic flux density which makes it an important parameter for fast switching times. As mentioned before, the most suitable framework for FFC air-cored magnet systems are cylindrical coils. But due to their finite length, the spatial field distribution of the magnetic flux density B is not homogeneous enough for the most FFC applications. There are various strategies described in the literature [9]-[12] which optimize the requirements of the magnet system. However, the optimization method of Schweikert et al. [10] has turned out to be the most suitable one for FFC magnet systems so far, while successfully translated for commercial use by a field-cycling system manufacturing company [13]. Besides the advantages of the Schweikert-type magnet system, there are some problems which might occur during the manufacturing process and when the magnet system suffers thermal stress. The complexity of the optimization process one has to master in order to obtain the non-uniform helix structure of the cut is not always straightforward. Another task is the fabrication method to cut the non-uniform helix structure(s) into the cylinder(s) with a reasonable precision. Due to the non-uniform helix of the magnet, the power dissipation over the magnet geometry under load is non-uniform distributed as well. Therefore, the thermal stress in the areas of the magnet with high current densities has to be minimized in a way that the magnet will not suffer any damages. Fig. 1 shows an example of a cylinder of a Schweikert magnet system as well as a possible power dissipation distribution of the whole geometry under an applied voltage.

This work was supported by Foncyt PICT2008-1810, CONICET PIP12200901000663, Mincyt Provincia de Córdoba and Secyt UNC.

S. Kruber, Universidad Nacional de Córdoba and IFEG-CONICET, kruber@famaf.unc.edu.ar.

G. D. Farrher, Universidad Nacional de Córdoba and IFEG-CONICET , gfarrher@famaf.unc.edu.ar

E. Anoardo, Universidad Nacional de Córdoba and IFEG-CONICET, anoardo@famaf.unc.edu.ar

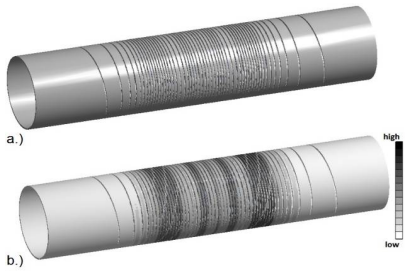

Figure 1. a.) Example of a cylinder of a Schweikert type magnet system. b.) Distribution of the power dissipation over the whole geometry.

II. Design Strategy

For a novel magnet system design, the idea was to develop a new system which is able to compensate changes in the magnetic flux density B and in the spatial homogeneity distribution $\Delta B / B$ during experimental use, which mainly occurs due to (small) geometrical changes of the magnet system. The reasons for these geometrical changes induced by mechanical stress are outlined above. Another source is deformations of the system due to long term usage. In order to compensate the negative effects of the geometrical changes of the magnet at operation, the current density must be adjusted or tuned accordingly. Such a correction system should be reactive on changes of the magnetic flux density B. It is obvious that this is not feasible with a Schweikert-type magnet system because once manufactured, the current density distribution along the coil(s) is fixed and not adjustable anymore. In order to obtain a magnet system with a "free tuneable current density distribution", the usage of one coil or various coils connected in series would not yield to the desired result, thus leading to the conclusion that such a system should be composed out of various independent coils. The general idea consists of a magnet system of several rings with rectangular cross section of the same size (see Fig. 2). These rings are collocated together in parallel and coaxial so that they form a cylinder with defined gaps between each ring. In order to reach a reasonable magnetic flux density B, by a certain applied electrical power P, the system is composed out of three cylinders (layers) which are arranged concentrically. Both inner layers, as well as the edge parts of the outer layer are connected in series and form the set of coils, called the *main coil*. All other parts (*elements*) of the outer layer have independent current controls. They are responsible for the generation of a low-intensity magnetic field which serves for

Figure 2. Magnet system composed out of n rings with a gap g between the rings. The dots symbolize the not shown rings between the 2nd and the (n-1)th ring.

the improvement of the homogeneity of the magnetic field within a region of interest. Fig. 3 is illustrating the arrangement of the three layer magnet system, where the dark areas symbolize the parts which are connected in series and the brighter areas the *elements* with an independent current control. Each part of the *main coil* as well as each *element* consists of a number of loops with rectangular cross-section (see Fig. 2).

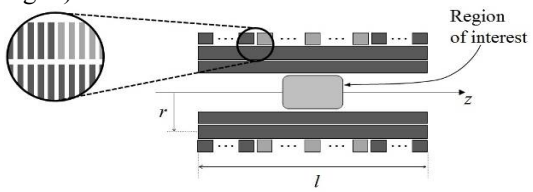

Figure 3. Illustration of the three layer magnet system from the xz-section plane.

III. Optimization Method

In order to optimize the homogeneity of the magnetic flux density $\mathbf{B}$ in a desired region of interest of the three layer magnet (Fig. 3), the system was divided into the *main coil* which generates the main magnetic field $\mathbf{B}^m$ and into the remaining *elements* which generate the low-intensity magnetic field $\mathbf{B}^h$ for the improvement of the homogeneity. Now the aim is to find the optimum number of elements with an appropriated set of currents $\{I_1,\ldots,I_N\}$ for the homogeneity improvement whereas the error between the magnetic field generated by the three layer magnet system and a *desired target magnetic field* B_z^t should be minimized. The set $\{I_1,\ldots,I_{N-1}\}$ corresponds to the currents of the *elements* and I_N to the current of the *main coil*. In order to find just one and not an infinite amount of solutions which lead to the same homogeneity, one has to impose more conditions. In this work, only one more condition is impossed: the power dissipation along the magnet system should be minimal as well. In order to determine the set of currents $\{I_1,\ldots,I_N\}$, the functional $U(I_1,\ldots,I_N)$ was used [14]:

$$U(I_1,\ldots,I_N)=\frac{1}{2}\sum_{k=1}^{K} w(\mathbf{r}_k)\left[B_z(\mathbf{r}_k)-B_z^t(\mathbf{r}_k)\right]^2+\alpha\sum_{n=1}^{N} R_n I_n^2 \qquad (1)$$

The first term of the equation, serves to reveal the minimum of the difference between the total magnetic field in z-direction, $B_z(\mathbf{r}_k)=B_z^m(\mathbf{r}_k)+B_z^h(\mathbf{r}_k)$, and the desired target field $B_z^t(\mathbf{r}_k)$. The second term stands for the power dissipated along the magnet system, where the factor $w(\mathbf{r}_k)$ is a weighting function depending on the spatial position and α is a weighting factor for the minimization of the power dissipation. Knowing that the magnetic field at the position $\mathbf{r}$ generated by a steady current is described the Biort-Savart's law, it was formulated with respect to the spatial coordinates $\mathbf{r}_k$:

$$B(\mathbf{r}_k)=\sum_{n=1}^{N} I_n c_n(\mathbf{r}_k)$$

The summation goes over all *elements* and the *main coil*, each carrying one of the current I_n. The coefficient $c_n(\mathbf{r}_k)$ is

defined as:

$$c_n(\mathbf{r}_k)=\frac{\mu_0}{4\pi}\left[\int\frac{d\mathbf{l}\times\mathbf{r}_k}{r_k^2}\right]_z \quad (2)$$

Then, the functional in (1) becomes:

$$U=\frac{1}{2}\sum_{k=1}^{K}w(\mathbf{r}_k)\cdot\left[I_n c_n(\mathbf{r}_k)-B_z^t(\mathbf{r}_k)\right]^2+\frac{\alpha}{2}\sum_{n=1}^{N-1}R_n I_n^2 \quad (3)$$

Note that the summation of the second term only goes to N-1. This is due to the fact that the power dissipation minimization is only done for the *elements* and not for the *main coil*. If the *main coil* is included into the summation, the currents of the *elements* would reach values comparable to that of the *main coil*. This is not desired because it would increase the amount of high power sources needed as well as it leads to a more complex cooling system of the FFC device. The set of currents $\{I_1,\ldots,I_N\}$ which minimizes the functional is found by differentiating it with respect to each variable I_n. In this way, a linear system of equations is obtained, here shown in a matrix:

$$(\mathbf{A}+\alpha\cdot\mathbf{R})\cdot\mathbf{I}=\mathbf{E} \quad (4)$$

where:

$$A_{nl}=\sum_{k=1}^{K}w(\mathbf{r}_k)c_n(\mathbf{r}_k)c_l(\mathbf{r}_k)$$

$$E_n=\sum_{k=1}^{K}w(\mathbf{r}_k)c_n(\mathbf{r}_k)B_z^t(\mathbf{r}_k)$$

By inverting this equation one can find the column vector $\mathbf{I}$ which contains the current values I_n. The coefficients $c_n(\mathbf{r}_k)$ in (2) were calculated numerically in C++, where the integral was discretized by replacing it with a summation. Geometrically, the discretization was done by dividing each loop into a finite number of thin rings. Afterwards these rings were divided once again in a finite number of segments of lenght *dl*, where each segment can be approximated by a filamentary line as shown in the Fig. 4. Now, if I is the current flowing through each loop, a current I / (n_r n_z) is carrying in each segment, where n_r is the number of divisions in the radial- and n_z is the number of divisions in the z-direction. The accuracy of the computed magnetic field rises as the number of n_r and n_z increases, but the time needed for the calculation process increases too. Due to that, an appropriate number of divisions had to be chosen.

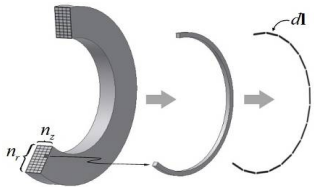

Figure 4. Discretization of one loop into a finite number of segments.

Once the coefficients $c_n(\mathbf{r}_k)$ are computed, the matrix $\mathbf{A}$ and the vector $\mathbf{E}$ from (4) were determined. The solution of (4) was achieved using C++ by inverting the matrix $\mathbf{A}$ with an algorithm based on the Gauss-Jordan elimination method.

Assuming that the current distribution is symmetric about the centre of the magnet system, the number of elements is chosen to be odd, since for an even number, the element pair about the centre of the magnet system would carry the same current and can be therefore replaced by just one element. With this assumption, the number of currents which has to be determined is reduced to $N/2+1$. The following figure shows, which current is assigned to each *element*.

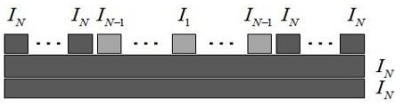

Figure 5. Assignment of the currents to each element.

The number of *elements* was varied from 7 to 19, whereas the number of parts, connected in series with the inner layers, of the outer layer of the *main coil* ranged from 0 to 3. The number of loops in each *element* plus in the *main coil* remained constant while varying the whole number of *elements* in the outer layer. For each number of *elements* chosen, the value of the weighting factor α was varied from 10^{-18} to 10^{-7}.

The region of uniformity is formed by all the coordinates $\mathbf{r}_k$ such that:

$$\frac{\Delta B_z(\mathbf{r})}{B_z(\mathbf{0})}\times 10^6\le\upsilon$$

where, $\Delta B_z(\mathbf{r})=B_z(\mathbf{r})-B_z(\mathbf{0})$, $B_z(\mathbf{0})$ is the magnetic field around the center of the magnet system and υ (in units of *part per million* or *ppm*), stands for the degree of the desired homogeneity. Therefore, the smaller the value of υ, the more homogeneous is the field.

Because the system posses azimuthal symmetry, it is sufficient to study the magnetic field in a plane parallel to the axis of the coil, for instance the xz-plane.

In order to find the optimal parameters of the magnet system, the area of the region with a homogeneity of 1ppm in the xz-plane was calculated.

However, as it is desired to keep the current intensity low for the *elements*, on one hand the spatial homogeneity of the magnetic field increases with the number of *elements*, on the other hand, the number of *elements* should be minimized due to the fact, that it would increase the number of independent power supplies needed for the FFC-device. Therefore, one has to search a compromise between the spatial homogeneity of the magnetic field, the intensity of the currents of the *elements* and the number of *elements*. By analyzing these results it was found, that the optimal number for the *elements* was 11 plus 2 parts at each edge of the outer layer for the formation of the *main coil*. Therefore, the number of currents which had to be determined were N=7. The current distribution for the whole magnet system, to reach a magnet flux density of $B=0.4T$ about the centre of it, is shown in Fig. 6. Where the grey dots symbolize the current intensity of the *main coil* and the black

squares symbolize which current is assigned to each *element*. Fig. 7 shows the calculated areas covering certain homogeneities in the xz-plane.

IV. FINITE ELEMENT METHOD SIMULATION

The Finite Element Method (FEM) has nowadays a widespread employment in the solution of scientific and engineering problems. In this work a commercial FEM program [15] for the calculation of the magnetic flux density was used in order to verify the results obtained from the optimization method discussed above. The geometry of the magnet system for the simulation was created, enclosed into an air sphere and afterwards cut by a symmetry operation by using the DesignModeler of the FEM program. For the analysis of the magnetic flux density B, the Analysis System "Magnetostatic" was chosen. Material parameters were adjusted and afterwards the creation of the mesh of the whole

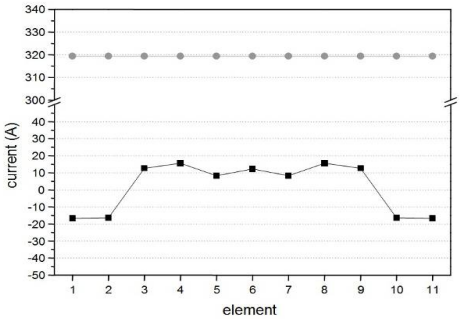

Figure 6. Current distribution for each *element* and the *main coil*.

geometry was done by using the defaults of the program. The same was done with the solver, all parameters were left untouched. Fig. 8 shows the mesh of the geometry. Together with the currents for each part of the magnet system, obtained by the optimization method before, the homogeneity $\Delta B / B$ was calculated by using the results of the magnetic flux density B from the FEM program for the xz-plane of the geometry. Fig. 9 shows the result obtained from the procedure mentioned above. The centre of the magnet system is located at the coordinates $x = 0mm$, $y = 0mm$, $z = 0mm$ and the corresponding magnetic flux density at this point was used as the reference for the calculation of $\Delta B / B$.

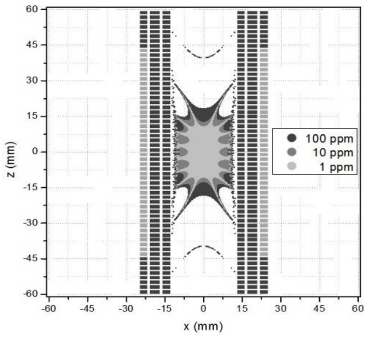

Figure 7. Calculated Areas with certain homogeneity of the magnetic field inside the magnet system.

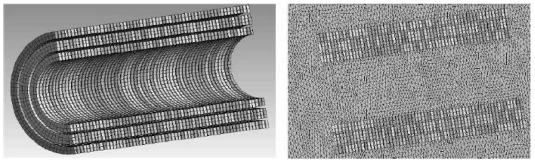

Figure 8. 3D Mesh of the magnet system cut by symmetry operations (left). 3D mesh of the magnet system incorporated into the 3D mesh of the surrounding air (right).

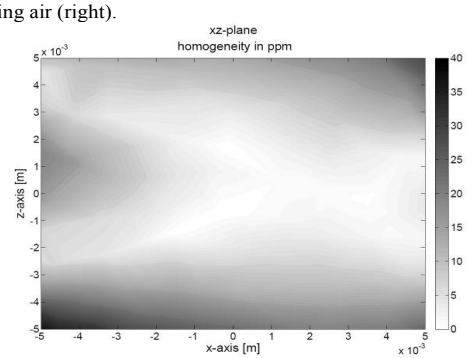

Figure 9. Map of the magnetic field distribution in ppm for the area of 10x10mm

Taking into account that the method used to verify the assumptions and the results obtained by the optimization method, gives approximated solutions, it is to say that the results show that it is possible to achieve a reasonable homogeneity in a desired volume with the results obtained through the optimization method.

Furthermore the simulation has shown that the magnetic flux density at the centre of the magnet system with the corresponding currents is $B = 0.395T$. This result is to 98.75% in agreement with the assumption of the optimization process.

V. DYNAMIC BEHAVIOR

Since the magnet flux density of the magnet system depends directly on the current flowing through it, it is essential to analyze the current distribution I of the whole circuit. For only one coil, which possesses an inductance L and a resistance R, connected with a switchable voltage source V_0, the time evolution of the current is given by [2]:

$$\frac{di(t)}{dt} = \frac{1}{L}\left(V_0 - i(t) \cdot R\right) \qquad (5)$$

If the magnet system contains more than one coil and each coil is controlled by a different voltage source, the calculus gets more complex. Fig. 10 shows the arrangement of the different electrical circuits for each coil.

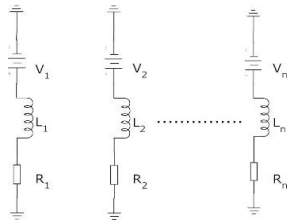

Figure 10. Electrical circuits for each coil

According to the Kirchhoff's mesh rule it leads to the following equation system:

$$0 = V_1(t) - R_1 \cdot i_1(t) - L_1 \frac{di_1(t)}{dt} - M_{21} \frac{di_2}{dt} - \ldots - M_{n1} \frac{di_n}{dt}$$
$$0 = V_2(t) - R_2 \cdot i_2(t) - M_{12} \frac{di_1(t)}{dt} - L_2 \frac{di_2}{dt} - \ldots - M_{n2} \frac{di_n}{dt}$$
$$\vdots$$
$$0 = V_n(t) - R_n \cdot i_n(t) - M_{1n} \frac{di_1(t)}{dt} - M_{2n} \frac{di_2}{dt} - \ldots - L_n \frac{di_n}{dt}$$

being *Mij* the mutual inductance between the different coils. This equation system can be rearranged to:

$$\begin{pmatrix} \frac{di_1(t)}{dt} \\ \vdots \\ \frac{di_n(t)}{dt} \end{pmatrix} = -\begin{pmatrix} \frac{L_1}{R_1} & \cdots & \frac{M_{n1}}{R_1} \\ \vdots & \ddots & \vdots \\ \frac{M_{1n}}{R_n} & \cdots & \frac{L_n}{R_n} \end{pmatrix}^{-1} \cdot \begin{pmatrix} i_1(t) \\ \vdots \\ i_n(t) \end{pmatrix} + \begin{pmatrix} \frac{L_1}{R_1} & \cdots & \frac{M_{n1}}{R_1} \\ \vdots & \ddots & \vdots \\ \frac{M_{1n}}{R_n} & \cdots & \frac{L_n}{R_n} \end{pmatrix}^{-1} \cdot \begin{pmatrix} \frac{V_1(t)}{R_1} \\ \vdots \\ \frac{V_n(t)}{R_n} \end{pmatrix}$$

or more compact:

$$\begin{pmatrix} \frac{di_1(t)}{dt} \\ \vdots \\ \frac{di_n(t)}{dt} \end{pmatrix} = -\mathbf{L}^{-1} \cdot \begin{pmatrix} i_1(t) \\ \vdots \\ i_n(t) \end{pmatrix} + \mathbf{L}^{-1} \cdot \begin{pmatrix} \frac{V_1(t)}{R_1} \\ \vdots \\ \frac{V_n(t)}{R_n} \end{pmatrix} \quad (6)$$

where $\mathbf{L}$ is the inductance matrix of the whole magnet system. Equation 6 has the form to proceed with the solution of the differential equations like it is reported in the literature [16]. The first step is to compute the fundamental matrix $\mathbf{F}$ of the homogeneous system, where the solution is $\mathbf{F}(t) \cdot \mathbf{c}$. In order to obtain the solution of the non-homogeneous system, the constant $\mathbf{c}$ is assumed to be a time dependent vector which has to be found with the following form:

$$\begin{pmatrix} c_1(t) \\ \vdots \\ c_n(t) \end{pmatrix} = \int \mathbf{F}(t')^{-1} \cdot \mathbf{L}^{-1} \begin{pmatrix} \frac{V_1(t')}{R_1} \\ \vdots \\ \frac{V_n(t')}{R_n} \end{pmatrix} dt' + \cdot \begin{pmatrix} k_1 \\ \vdots \\ k_n \end{pmatrix}$$

where $\mathbf{k}$ is an arbitrary additive constant. Now substituting the vector $\mathbf{c}(t)$ into (6) results in the solution of the dynamic behaviour of the magnet system:

$$\begin{pmatrix} i_1(t) \\ \vdots \\ i_n(t) \end{pmatrix} = \mathbf{F}(t) \cdot \begin{pmatrix} k_1 \\ \vdots \\ k_n \end{pmatrix} + \mathbf{F}(t) \int \mathbf{F}(t')^{-1} \cdot \mathbf{L}^{-1} \begin{pmatrix} \frac{V_1(t')}{R_1} \\ \vdots \\ \frac{V_n(t')}{R_n} \end{pmatrix} dt' \quad (7)$$

The constants inside the vector $\mathbf{k}$ are found by using any initial condition. In order to terminate with the computation one has to set the distributions for the voltages $V_1(t), V_2(t), \ldots, V_n(t)$. This is usually done by the experimenter and depends on the voltage sources in use.

VI. Magnet System Characteristics

Once the simulations have shown that a reasonable homogeneity in a desired volume as well as sufficient high magnetic flux density can be achieved by the magnet system, the focus lays on the variation rates of the magnetic field dB/dt. Like it was already mentioned, the variation rates depend directly on the inductance and the resistance of each element of the magnet system. In order to obtain the self- and mutual-inductance of each element various approaches were used. More precisely, for the self-inductance of one ring the approaches of Yu et al. [17] and Babic et al. [18] and for the mutual inductance between the rings the one of Kim et al. [19]. For the calculation of the resistances of each element the well known equation was used:

$$dR = \rho \cdot \frac{dl}{dA}$$

This gives the following expression for a conductor with the geometry used in this work:

$$R = \frac{2\pi \cdot \rho}{x \cdot \ln\left(\frac{R_2}{R_1}\right)}$$

Where ρ is the specific resistance of the material of the ring, x stands for the width of the ring and R_1 and R_2 are the inner and outer radii of the loop. The resistances for each element were calculated by using the dimension of each ring, calculating the corresponding resistance (specific resistance of copper at $T = 293.15K$) and multiplying them by the number of rings one part contains. The results for the inner coils (main coil) and for one element of the outer coils (element 1 to 11) are: $R_1 = 0.0339\Omega$, $R_2 = 0.0339\Omega$, $R_{3,\ldots,17} = 0.0036\Omega$. The resistances of each part together with the inductances (see Fig. 11) form the matrix L in (5). Due to the idea, that the inner layers and the two elements of both edges, from the outer layer, are connected in series, the matrix changes from a $17x17$ to a $12x12$ matrix. The parts mentioned above form the *main coil* and the elements 1-11. If the voltages $V_{maincoil}$, $V_1 \ldots V_{11}$ are switched instantaneously from $0V$ to the value needed to reach the determined current of each part (see Fig. 6), each part of the magnet system will have a current behaviour calculated by (6) and shown in the Fig. 12. This dynamical behaviour of all parts leads to a switching time of the whole magnet system, from $B(0) = 0T$ to $B(t_{final}) = 0.4T$, in $t \approx 20ms$.

Figure 11. Numeration of each part.

VII. Conclusion

It was shown that it is feasible, with the methods (optimization method, FEM Simulation) shown in this work, to design a magnet system for FFC usage with a novel homogeneity control, without violating other requirements such as field variation rates dB/dt as well as maximal magnetic flux density B.

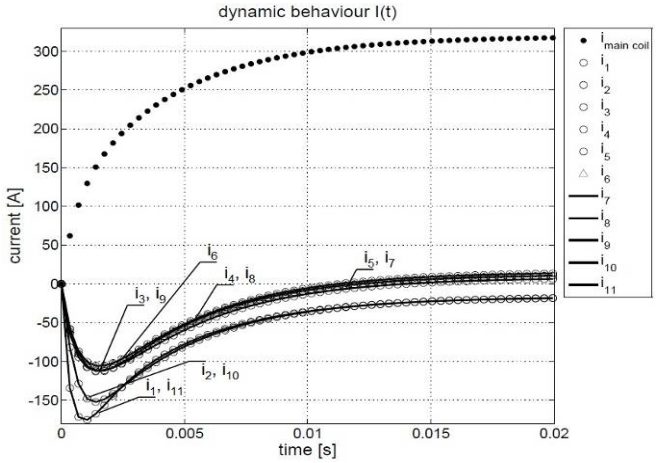

Figure 12. Dynamic behaviour of each element (above). Dynamic behaviour of the total magnetic flux density around the center of the magnet system.

REFERENCES

[1] E. Anoardo, G. Galli, and G. Ferrante. "Fast-Field-cycling NMR: Applications and Instrumentation". *Applied Magnetic Resonance*, 20:365-404, 2001.

[2] Rainer Kimmich; Esteban Anoardo. "Field-cycling NMR relaxometry". *Progress in Nuclear Magnetic Resonance Spectroscopy*, 44:257-320, 2004.

[3] Gianni Ferrante and Stanislav Sykora. "Technical Aspects of Fast Field Cycling". *Advances in Inorganic Chemistry*, 57: 405-470. Academic Press, 2005.

[4] J.W. Carlson, D.M.Goldhaber, A. Brito, L.Kaufman. "MR Relaxometry Imaging". *Radiology*, 184:635-639, 1992.

[5] N.I. Matter, G.C. Scott, T. Grafendorfer, A. Macovski, S. M. Conolly. "Rapid Polarizing Field Cycling in Magnetic Resonance Imaging". *IEEE TRANSACTIONS ON MEDICAL IMAGING*, VOL. 25, NO. 1, JANUARY 2006

[6] D.J. Lurie, S. Aime, S. Baroni, N. A. Booth, L. M. Broche, C-H. Choi, G. R. Davies, S. Ismail, D. Hogain, K. J. Pine. "Fast field-cycling magnetic resonance imaging". *Comptes Rendus Physique*, 11: 136-148,2

[7] D.J. Lurie, M. A. Foster, D. Yeung, J. M. S. Hutchison. "Design, construction and use of a large-sample field-cycled PEDRI imager". *Phys. Med. Biol*, 43: 1877-1886, 1998

[8] D.J. Lurie, G. R. Davies, M. A. Foster, J. M. S. Hutchison. " Field-cycled PEDRI imaging of free radicals with detection at 450 mT". *Magnetic Resonance Imaging*, 23 : 175–181, 2005

[9] G.Grössl, F. Winter and R. Kimmich. "Optimisation of magnet coils for NMR Field cycling experiments". *J. Phys. E*: Sci. Instrum., 18:358-360, 1985.

[10] K.H Schweikert, R Krieg, and F Noack. "A high-Field air-cored magnet coil design for fast-field-cycling NMR". *Journal of Magnetic Resonance* (1969), 78(1):77-96, 1988.

[11] O. Lips, A.F. Privalov, S.V. Dvinskikh, and F. Fujara. "Magnet Design with High B0 Homogeneity for Fast-Field-Cycling NMR Applications". *Journal of Magnetic Resonance*, 149(1):22-28, 2001.

[12] Dirk Plendl, Marian Fujara, Alexei F. Privalov, and Franz Fujara. "Energy efficient iron based electronic field cycling magnet". *Journal of Magnetic Resonance*, 198(2):183-187, 2009.

[13] Stelar s.r.l., *Via Enrico Fermi, 4 - 27036 MedePavia, (PV) - Italy*, www.stelar.it.

[14] M. Poole and R. Bowtell, "Novel Gradient Coils Designed Using a Boundary Element Method", *Concepts in Magnetic Resonance* Part B: Magnetic Resonance Engineering, 31B, 162-175, (2007).

[15] ANSYS 13, http://www.ansys.com/Products/ANSYS+13.0+Release+Highlights ANSYS Inc., *Southpointe 275 Technology Drive Canonsburg, PA 15317*.

[16] William E. Boyce and Richard C. DiPrima. "Elementary Differential Equations and Boundary Value Problems". *John Wiley & Sons, Inc., 7th edition, New York 2001*. Page: 411-415

[17] Dingan Yu and K. Han. "Self-inductance of air-core circular coils with rectangular crosssection.", *IEEE Transactions on Magnetics*, 23(6):3916-3921, Nov. 1987.

[18] S. Babic and C. Akyel. "Improvement in calculation of the self- and mutual inductance of thin-wall solenoids and disk coils". *IEEE Transactions on Magnetics,* 36(4):1970-1975, July 2000.

[19] Ki-Bong Kim, E. Levi, Z. Zabar, and L. Birenbaum. "Mutual inductance of noncoaxial circular coils with constant current density." *IEEE Transactions on Magnetics*,33(5):4303-4309, Sep. 1997.

Stephan Kruber received the engineering degree in engineering physics from Ilmenau University of Technology - Ilmenau, Thüringen, Germany, in 2009, and is a PhD student in physics at the Universidad Nacional de Córdoba (UNC), Córdoba, Argentina. His current research interests are Fast-Field-Cycling NMR and Fast-Field-Cycling MRI.

Germán David Farrher received the PhD in Physics from Universität Ulm, Ulm, Germany. He has been working for the Argentinas CONICET as a researcher since 2007. He is Professor at UNC since 2007. His current research interest includes magnetic fields control for FFC-NMR applications.

Esteban Anoardo Anoardo received the PhD. degree in physics from Universidad Nacional de Córdoba (UNC-Argentina) in 1990. He holds a Professor position at FaMAF - UNC where he leads the LaRTE lab. His research interests include a mix of NMR hardware and its applications in selected topics. He is fellow of CONICET at the Enrique Gaviola Physics Institute. He also serves on the Director Board of the technology incubator of Famaf (IEBTF).